Microstructured, Functional PVA Hydrogels through Bioconjugation with Oligopeptides under Physiological Conditions

*Siow-Feng Chong, Anton A. A. Smith, and Alexander N. Zelikin**

In this work, bioconjugation techniques are developed to achieve peptide functionalization of poly(vinyl alcohol), PVA, as both a polymer in solution and within microstructured physical hydrogels, in both cases under physiological conditions. PVA is unique in that it is one of very few polymers with excellent biocompatibility and safety and has FDA approval for clinical uses in humans. However, decades of development have documented only scant opportunities in bioconjugation with PVA. As such, materials derived thereof fail to answer the call for functional biomaterials for advanced cell culture and tissue engineering applications. To address these limitations, PVA is synthesized with terminal thiol groups and conjugated with thiolated peptides using PVA in solution. Further, microstructured, surface-adhered PVA physical hydrogels are assembled, the available conjugation sites within the hydrogels are quantified, and quantitative kinetic data are collected on peptide conjugation to the hydrogels. The success of bioconjugation in the gel phase is quantified through the use of a cell-adhesive peptide and visualization of cell adhesion on PVA hydrogels as cell culture substrates. Taken together, the presented data establish a novel paradigm in bioconjugation and functionalization of PVA physical hydrogels. Coupled with an excellent safety profile of PVA, these results deliver a superior biomaterial for diverse biomedical applications.

1. Introduction

Communication between a cell substrate and adhering cells is a multilingual process that relies on the vocabulary of chemistry, physics and geometry, each providing opportunities to fine-tune the performance of intelligent biointerfaces.[1–3] Cell adhesion,[4] proliferation,[5] migration[6] and even intracellular processes and metabolic state[7,8] as well as success of drug delivery to cultured cells[9] are all under effective control elicited by the properties of a biomaterial. The latter include fouling behavior of the surface,[5] specific biorecognition and/or therapeutic cues, matrix elasticity,[4,10,11] and surface topography.[12,13] This notion illustrates a pivotal role of designer interfaces towards successful cell culture and particularly tissue engineering (TE). Specifically, micro-structured (μS) and micro-patterned substrates have proven to be highly important for culture and co-culture of mammalian cells towards e.g. cell patterning, drug screening, engineering of multi-cell type tissues etc.[14–20] Among diverse candidate materials for these undertakings, hydrogels appear to be unique in that the matrices comprised thereof offer rationally designed Young's moduli[2,3] and mimic diverse human tissues.[2,21] Using hydrogels, it is therefore possible to construct interfaces with independent control over all of the aforementioned cues, including elasticity.

Towards this end, we have recently reported on nano- and micro- structured hydrogels based on poly(vinyl alcohol), PVA,[22–26] a polymer with an excellent history of

Dr. S.-F. Chong, A. A. A. Smith, Prof. A. N. Zelikin
Department of Chemistry
Aarhus University
Aarhus C, 8000, Denmark
E-mail: Zelikin@chem.au.dk

DOI: 10.1002/smll.201201774

small NANO MICRO

biomedical applications, specifically TE.[27,28] In our work, we focused on physical hydrogels, i.e. three dimensional polymer networks with junction knots comprised of non-covalent linkages, namely hydrogen bonds and Van der Waals interactions. Towards creation of intelligent biointerfaces, we developed surface-adhered PVA physical hydrogels with micro- and nanoscale topography design,[23] tunable Young's modulus,[22,24] and controlled cell adhesion.[22] We developed polymersome-loaded "composite" hydrogels as drug eluting biointerfaces and revealed that delivery of anti-cancer depsipeptide mediated by the hydrogels to adhering cells was more efficient than achieved via solution based administration of the drug.[26] We then introduced Substrate Mediated Enzyme Prodrug Therapy, a novel concept in drug delivery wherein active therapeutic is synthesized from externally administered benign prodrugs by the enzyme within the hydrogel phase for delivery to adhering cells and surrounding tissues.[25] However, a persistent shortcoming of biomaterials based on PVA remains unsolved, namely scant opportunities in bioconjugation and hydrogel functionalization in particular.[29] In their current form, PVA hydrogels largely fail to answer the call[30–32] for enhanced drug delivery opportunities engineered into the matrices for TE. In this work, we specifically address this issue and develop bioconjugation of peptides to PVA under physiological conditions using both, polymer in solution and within the structure of μS hydrogels.

PVA is the largest water-soluble polymer produced worldwide,[33] with decades of development and broad utility in biomedicine including clinical applications.[29,34] This polymer was used to deliver one of the first documented successes of polymer–protein conjugates with improved pharmacokinetics.[35] However, while numerous studies considered bioconjugation to PVA,[29] techniques for site-specific conjugation to PVA through polymer terminal groups are solitary.[36] Chain-end bioconjugation is particularly important in the context of e.g. polymer-protein conjugates and 7 out of 9 FDA-approved protein conjugates with PEG use this strategy for conjugation.[37] In recent years, developments in atom transfer radical polymerization (ATRP) and particularly reversible addition-fragmentation chain-transfer (RAFT) polymerization chemistries delivered opportunities in controlling polymer terminal groups.[38,39] However, these techniques for macromolecular design using PVA are largely futile: PVA is typically obtained via saponification of a precursor polymer (e.g., polyvinyl acetate), a step that is expected to obliterate most terminal groups employed for bioconjugation purposes. For RAFT derived polymers, conversion of a terminal thioester into thiol functionality is poised as a reliable and uniform approach to bioconjugation,[40,41] yet this strategy too fails to accommodate PVA for which side reactions result in loss of terminal thiols.[42] Recently, we described an approach to macromolecular design of PVA using RAFT polymerization technique and a chain transfer agent with an "R" group containing phthalimide functionality.[43] This strategy afforded polymers with judiciously chosen molecular weights and terminal amine groups upon cleavage of phthalimide protecting group. Amine functionality is significantly advantageous in comparison to PVA hydroxyls for site-specific bioconjugation reactions using a suit of well-established biocompatible chemistries.

From a different perspective, conjugation reactions that are compatible with fragile biological cargo are also imperative for functionalization of hydrogels and PVA hydrogels in particular. Typical approaches to chemical stabilization of hydrogels based on PVA as well as immobilization of cargo into the hydrogel bulk or onto the surface employ harmful, non-specific chemicals, e.g., glutaraldehyde. This may lead to a loss of function for immobilized cargo[44] and toxic effects to the adhering cells.[45] A number of alternative, benign conjugation strategies were described for conjugation with PVA in solution,[29] however, with rare exceptions[46,47] these were not implemented for hydrogel materials derived thereof.

In this work, to address the above-mentioned challenges, we build on success of our report on the synthesis of PVA via RAFT polymerization and establish a synthesis of PVA with terminal thiol groups. Of different bioconjugation methodologies, thiol-disulfide interconversion stands out as a reaction with excellent specificity to thiols and mild reaction conditions. Reversible nature of this linkage also places this chemistry among the most warranted in the context of intracellular drug delivery.[48] Further to this, in a form of a mixed disulfide with, e.g., thiopyridine or Ellman reagent, the thiol is protected from oxidation and other side reactions and is activated towards thiol-disulfide reshuffling, i.e. bioconjugation.[41] Finally, a possibility to track the progress of the latter conversion via UV-vis spectroscopy makes this chemistry unique for facile quantitative tests and measurements.

The choice of oligopeptides as model cargo was made with an aim of developing μS PVA hydrogels towards their use in TE and advanced cell culture applications. Oligopeptides are among the most diverse and potent bioactive molecules. Depending on the structure, oligopeptides orchestrate immunity[49] and inflammatory responses,[50] have anti-cancer,[51] antiviral,[52] and antimicrobial effect,[50] can be used for directed cell adhesion[13] etc, all of which is important in the context of TE and justifies importance of the results presented below. Together with our prior reports,[22–26] this work established μS physical PVA hydrogels as a novel platform with multi-armed control over the properties of both, interface and matrix bulk, towards enhanced opportunities in communicating with adhering cells.

2. Results and Discussion

To obtain PVA amenable for thiol-disulfide exchange, a polymer sample was synthesized via RAFT using *O*-ethyl, *S*-phthalimidomethyl xanthate RAFT agent, deprotected using hydrazine into amine-terminated chains,[43] and further reacted with Traut's (2-iminothiolane) and Ellman's reagents (ER), **Figure 1**. The latter conversion was accomplished in a single step without purification of the thiolated polymer. For polymer characterization and to verify the success of this reaction, we employed gel permeation chromatography (GPC) with a multi-angle light scattering (MALS) and a full spectrum UV-vis photo diode assay detector, **Figure 2**. Analysis of modification of polymer end groups is complicated in that minor impurities of e.g. ER are significant and possibly dominate UV spectra of the polymers. Further to this, solution of

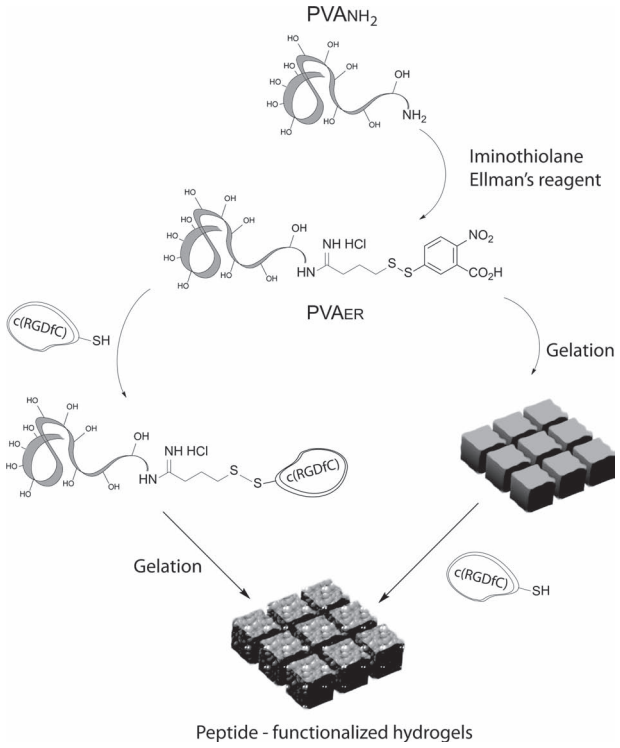

Figure 1. RAFT-derived PVA with terminal amine groups (PVA_{NH2}) was converted into thiol-functionalized PVA (PVA_{ER}) through a one-step functionalization using Traut's and Ellman's reagents and resulting polymer was employed to assemble µS physical hydrogels. Functionalization of hydrogels with oligopeptides was achieved via two routes, namely (i) solution-phase bioconjugation followed by assembly of µS physical hydrogels and (ii) introducing function into µS physical hydrogels via conjugation of the peptides to gel forming polymer chains.

a mixture of polymer and ER will reveal the same spectrum as a polymer chain after successful conversion with Traut's/ER. In contrast, a combination of MALS and UV detectors provides unequivocal proof of the end group conversion. Elution volume corresponding to the polymer (Figure 2) bears a UV signature of the ER (λ_{max} = 334 nm) and thus confirms end-group conversion. A shift in the maximum on the elution volume axis observed on a pseudo-3D plot as compared

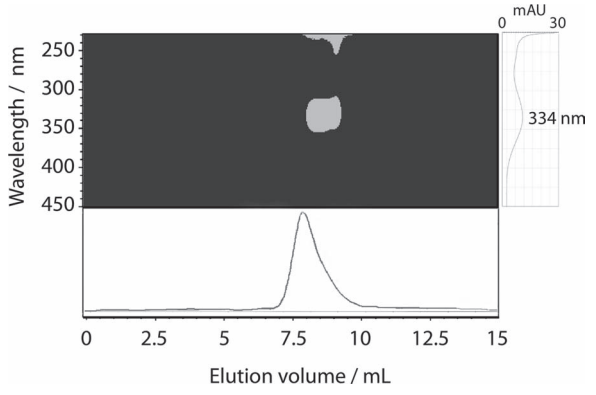

Figure 2. Results of GPC analysis of PVA_{ER} using a combination of multi-angle light scattering and a full spectrum UV-vis photo diode assay detectors.

to the MALS elution profile is readily explained by an increasing mole fraction of terminal groups in shorter polymer chains, the latter eluting at progressively later times. In optimizing modification of PVA terminal groups and product isolation, we observed that desalting (size exclusion) columns do not provide exhaustive removal of ER and byproducts of the outlined chemical reaction. Instead, polymer isolation via precipitation into methanol followed by trituration with this solvent proved to be a suitable polymer isolation approach. Quantification of the terminal groups using UV-vis spectrum and comparing M_n values derived thereof to those obtained from GPC analysis reveal ca. 80% yield of terminal group conversion.

Hydrogel biomaterials find extensive use in biotechnological and biomedical applications.[53–56] However, compared to other materials, hydrogels suffer from poor methods available for their characterization. To address this challenge, recently we developed a micro-transfer molding (µTM) technique to produce surface-adhered PVA hydrogels which are amenable for visualization using light/differential interference contrast (DIC) microscopy techniques and allow detailed characterization using atomic force microscopy (AFM) and force-distance measurements.[22,23] We provided first attempt to quantify "assembly losses", i.e. quantify polymer chains that escape gelation and are registered in bulk solution, i.e. supernatant.[24,22] In the context of peptide cargo and immobilization of PVA bioconjugates as hydrogels, such quantification is imperative and serves as basis for a reliable estimate of the deliverable payload. Same holds true for conjugation of peptides to the polymer chains in the gel phase for which undertaking this analysis will enumerate the available conjugation sites. ER-modified PVA as developed above lends itself for quantification of polymer chains and available sites for bioconjugation. Below, we detail a novel approach to achieve this, specifically using PVA_{ER} and facile thiol-disulfide exchange with dithiothreitol (DTT), a fast, quantitative reaction.

µS PVA hydrogels were assembled via µTM using PDMS stamps with 2 µm-cuboid features and a non-cryogenic stabilization using 1 M sodium sulfate (Na_2SO_4) (1 h).[22] Briefly, solution of PVA was clamped between a PDMS stamp and a glass cover slip for 24 h at finger tight pressure. This results in a partial dehydration of the polymer and, upon detachment from PDMS stamp, yields surface-adhered PVA thin films. These materials dissolve upon contact with aqueous solutions and for polymer hydrogelation require a treatment with coagulating kosmotropic salt, Na_2SO_4. In this work, stabilizing salt solution, subsequent phosphate buffered saline (PBS) washes, and resulting µS hydrogels were analyzed for the presence of PVA, specifically through quantification of the terminal groups. To achieve this, collected solutions/hydrogel samples were charged with excess DTT to release 2-nitro-5-mercaptobenzoic acid (TNB) chromophoric group which was quantified using UV-vis spectroscopy, **Figure 3**. Presented data reveal that ca. 20% of the polymer chains taken for production of µS hydrogels escape gelation and are solubilized by the coagulating Na_2SO_4 solution. Subsequent washing with physiological buffer leads to a further release of the polymer which cumulatively enumerates to ca. 30% of the load, and resulting µS hydrogel samples contain ca. 50%

small NANO MICRO

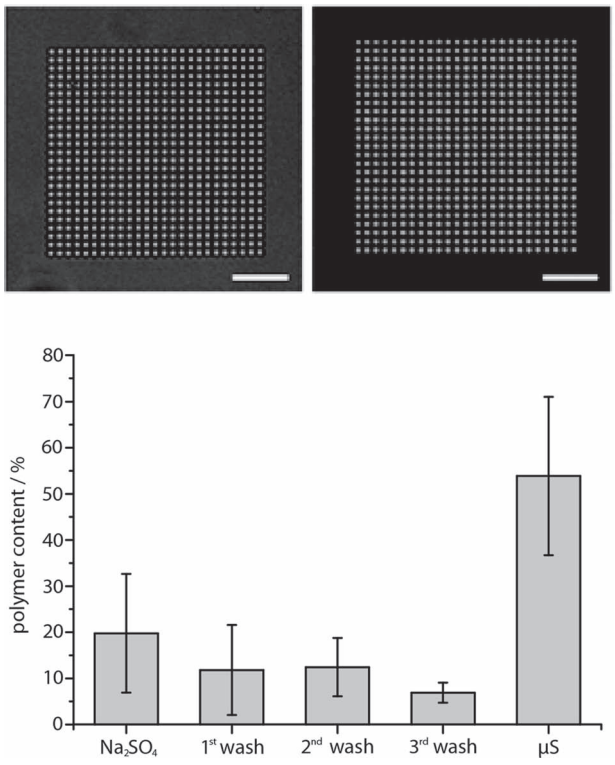

Figure 3. Top: DIC (left) and fluorescence (right) microscopy images of μS PVA films. Scale bars: 25 μm. Bottom: Quantification of PVA_{ER} in the coagulation bath (sodium sulfate), subsequent PBS washes and resulting μS hydrogels.

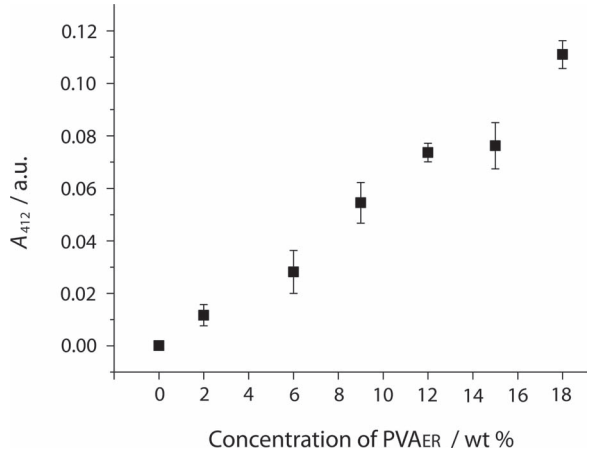

Figure 4. Thiol content within μS hydrogels as a function of concentration of PVA_{ER} employed for the hydrogel assembly. Thiol content is expressed via absorbance of TNB chromophore (λ_{max} = 412 nm) which is released from the polymer chain ends with addition of DTT.

of the polymer initially used in the assembly of μS hydrogels. We note that these numbers are in close agreement with our previous report in which we used fluorescently labeled 'reporter' PVA chains,[22] a notion which speaks towards creditability of the technique developed above. Suitability of this approach to quantification of polymer chains and conjugation sites is further substantiated by that all the readings cumulatively add up, with experimental error, to ca. 100%, i.e., a total amount of the polymer used for production of the μS hydrogels.

Having established a method to quantify incorporation of polymer chains into the hydrogel matrices, we next aimed to gain control over the number of available conjugation sites. We hypothesized that this can be achieved through a variation of polymer concentration used to produce μS matrices. To test this, PVA hydrogels were assembled using polymer samples in a range of concentrations from 2 to 18 wt% and a stabilization using 1 M Na_2SO_4. Resulting hydrogels were then treated with DTT, and liberated TNB was quantified using UV-vis spectroscopy. Resulting spectra showed a linear increase in the absorbance at 412 nm with increasing polymer concentration in the assembly solution, **Figure 4**. These data demonstrate an excellent degree of control over thiol content in the gel phase exerted through a judicious choice of the polymer concentration.

Surprisingly, analysis of polymer losses associated with the assembly of μS hydrogels revealed no statistically significant variation between samples and for all polymer concentration it was found to be ca. 50% (data not shown). We have previously shown that at a constant polymer concentration, assembly losses were significantly different between μS PVA hydrogels prepared via several non-cryogenic techniques, i.e., the use of kosmotropic salt, aqueous isopropanol or oligomeric (liquid) ethylene glycol.[22] Together with the data presented herein, these observations suggest that a fraction of polymer lost during hydrogel assembly is to a greater degree defined by a stabilization technique whereas polymer concentration has only a secondary role, at least within the studied range of polymer content.

Next, we aimed to gain control over available sites for conjugation independent from the overall content of the polymer in the matrix. The latter is expected to define such properties of the hydrogel as matrix elasticity and stability to degradation. For an independent control over each of these characteristics, it is therefore essential to decouple availability of the conjugation sites from the total polymer mass. To achieve this, thiol-activated PVA (PVA_{ER}) was mixed with parent amine-functionalized PVA (PVA_{NH2}) at varied ratios of the two polymers and keeping total polymer concentration of 12 wt%. These mixtures were then used in the preparation of μS hydrogels, and thiol content in each sample was determined as described above. Amount of available sites for conjugation increased linearly with the fraction of PVA_{ER} in the polymer mixture (**Figure 5**, top), which illustrates the desired independent control over total polymer content in the gel and thiol concentration. To demonstrate that the two methods of controlling thiol concentration in the gel phase are complimentary, two data sets (Figures 4 and Figure 5, top) were re-evaluated to present the total thiol content as a function of PVA_{ER} moles, a metric that is independent of the method used for preparation of the hydrogel. The two data sets superimpose onto a single linear curve (Figure 5, bottom), a notion that verifies reproducibility of the μTM for the preparation of μS PVA hydrogels. More importantly, it illustrates control exerted by μTM and the methods developed above over availability of conjugation sites and achieved independent polymer content in the hydrogel.

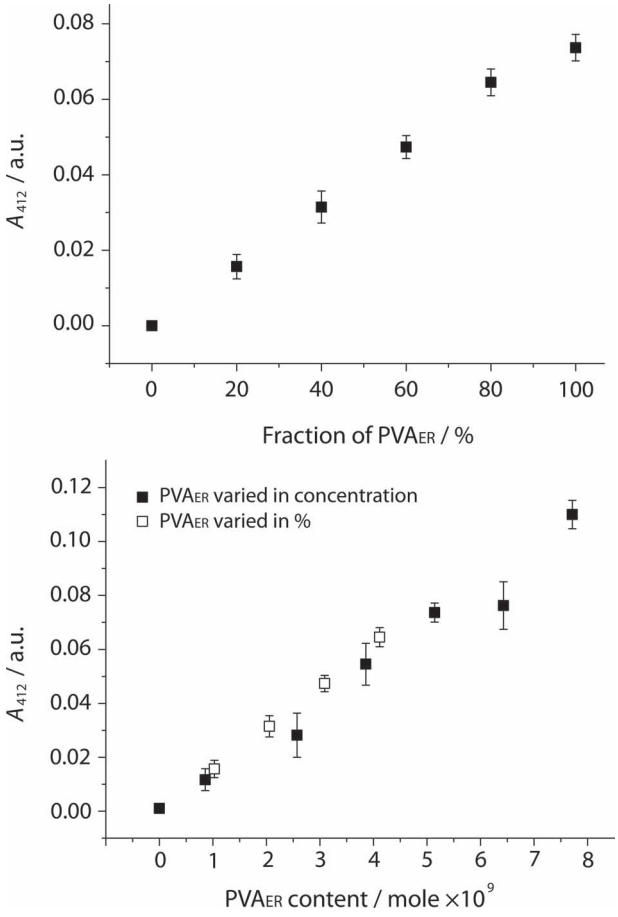

Figure 5. Top: Thiol content within μS hydrogels as a function of concentration of PVA_{ER} in a mixture with PVA_{NH2} employed for the hydrogel assembly. Bottom: thiol content within μS hydrogels as a function of absolute content of PVA_{ER} in solutions employed for the hydrogel assembly. For both graphs, thiol content is expressed via absorbance of TNB chromophore (λ_{max} = 412 nm) released from the polymer chain ends with addition of DTT.

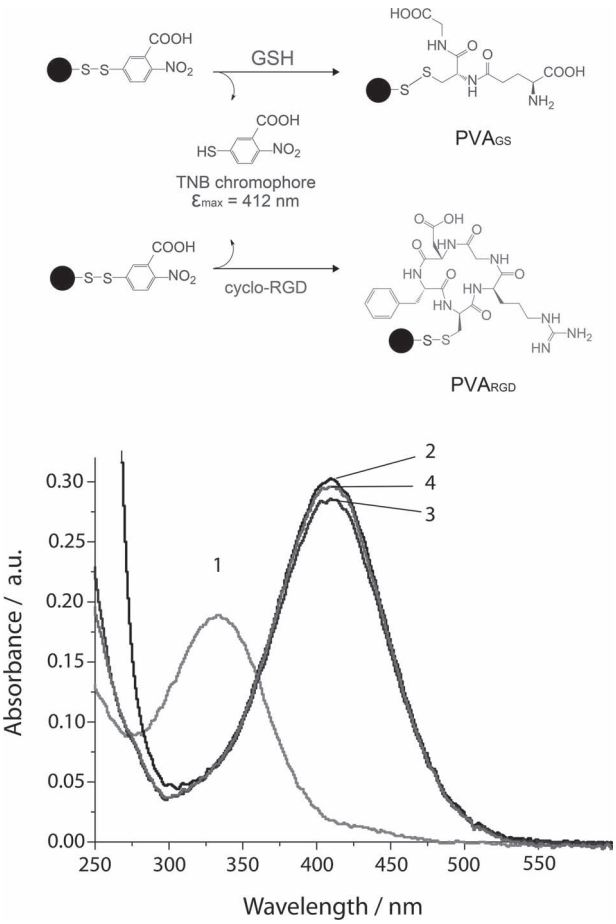

Figure 6. Top: Schematic illustration of the preparation of GSH-conjugated and RGD-conjugated PVA via thiol-disulfide exchange. Bottom: UV-spectra of aqueous solution of PVA_{ER} (1), solutions of mixtures of PVA_{ER} with excess DTT (2), GSH at a molar ratio of polymer: peptide of 1:1 (3) and c(RGDfC) at a molar ratio of polymer:peptide of 1:1 (4).

Oligopeptides constitute a broad class of compounds with diverse therapeutic effects, from anticancer and antiviral to immunostimulatory, (pro/anti) inflammatory, etc. In this work, to develop oligopeptide conjugation to PVA we used a natural thiol-containing tripeptide, glutathione (GSH), which is present in mammalian cells in millimolar concentrations. Further to this, to evaluate success of bioconjugation through a measurable function, we used an oligopeptide with thorough prior characterization and facile screen for activity, namely RGD.[57] This pro-cell adhesion tripeptide is highly specific with a loss of function observed on scrambled sequences and even with single amino-acid variants. Its function, promoting cell adhesion, is easily visualized using mammalian cells and methods of microscopic characterization. Whereas PVA has a well-documented low cell-adhesive nature,[29] conjugation with RGD is expected to render the hydrogels well suited to support adhesion of mammalian cells. This phenomenon would verify the success of bioconjugation and pave the way to conjugation of oligopeptides with diverse functions.

For conjugation in solution phase, a pH 8.3 carbonate buffer solution of PVA_{ER} was mixed with excess DTT, equimolar GSH, or commercially available thiol-containing derivative of RGD, c(RGDfC). UV-vis spectra of the mixtures were registered upon a 2 h incubation. For all the samples, within the specified incubation time reactions proceeded to high conversions, **Figure 6**. Assuming that with excess DTT thiol-disulfide reaction reached completion, peptide conjugation reactions reached ca. 85% conversions thus verifying a high efficiency of the proposed conjugation strategy.

The rationale behind employing RGD as a model peptide to elaborate on methods of bioconjugation with PVA is that this oligopeptide has an exhaustive documented characterization and a function which can easily be visualized, namely cell adhesion. Together with a low fouling nature of PVA, this provides for a convenient method of analysis on bioconjugation. μS hydrogels were prepared using commercial PVA, RAFT-derived PVA with terminal amine (PVA_{NH2}) and ER-groups (PVA_{ER}), as well as GSH-(PVA_{GS}) and c(RGDfC)- conjugated (PVA_{RGD}) polymer samples and then used as substrates

small NANO MICRO

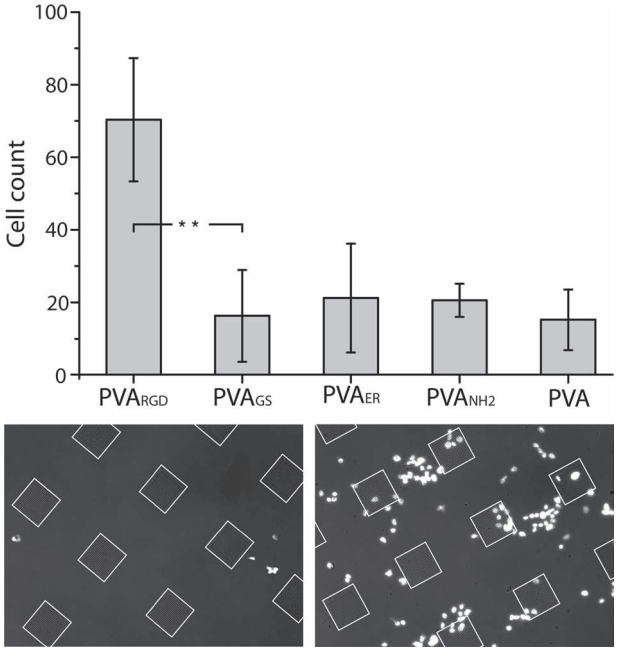

Figure 7. Top: Experimental values of cell counts of HepG2 cells cultured on μS PVA films. The data are presented as mean values (triplicates) ± SD (n = 3). ** is $p < 0.05$. Bottom: Fluorescence microscopy images of DAPI-stained HepG2 cells cultured on μS PVA$_{GS}$ (left) and PVA$_{RGD}$ (right) hydrogels. Scale bars are 100 μm.

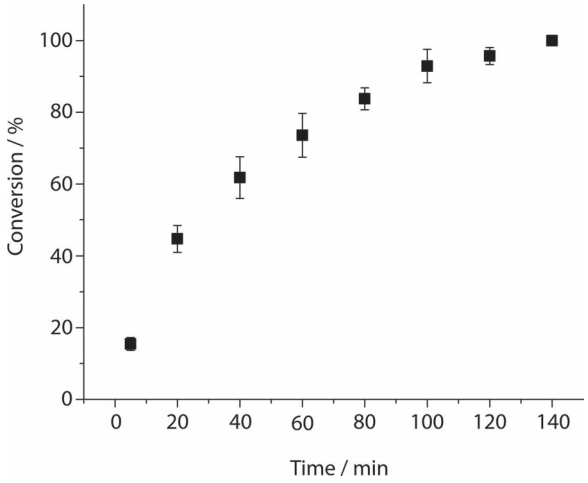

Figure 8. Kinetic profile for bioconjugation of GSH with PVA$_{ER}$ within hydrogel phase at a peptide to polymer molar ratio 2:1.

for adhesion and proliferation of hepatocellular carcinoma (HepG2) cells. Following a 24-hour attachment, the cells were fixed using paraformaldehyde (PFA), underwent a nucleus staining using DAPI, and were imaged using a fluorescent microscope. Resulting images were used to quantify cell adhesion via direct cell count, (**Figure 7**). As expected, pristine PVA hydrogels as substrates for cell adhesion exhibited a low cell count, i.e. sustained minor cell adhesion. Similarly, PVA$_{NH2}$ and PVA$_{ER}$ custom made polymers revealed minor cell counts, which were only marginally higher than that of pristine PVA. PVA$_{GS}$ bioconjugate also promoted minor cell adhesion and the samples derived thereof exhibited cell counts similar to pristine PVA. In contrast to all that mentioned above, PVA$_{RGD}$ bioconjugate formulated into μS hydrogels revealed a pronounced, statistically significant increase in the cell count revealing a success in bioconjugation and assembly of μS thin films using polymer-peptide conjugate. We note that hydrogels as employed herein were not uniform PVA matrices but μS surfaces spaced by non-structured areas of flash layer. While stability of the latter as such falls beyond the scope of this investigation, its (partial) dissolution will compromise the uniformity of a low fouling PVA thin film. We hold this phenomenon responsible for a non-negligible cell count observed on the samples prepared using pristine PVA. We further note that c(RGDfC) was used herein as a model peptide with an easily quantifiable function. The conjugation method described above is applicable to peptides with diverse structure and therapeutic function. Thiol-free peptides can be end-functionalized with an additional terminal cysteine to make these amenable for disulfide conjugation, as we have shown recently on oligopeptides for vaccination applications.[58] We anticipate that the proposed technique to functionalization of PVA hydrogels will lead to broader biomedical applications of this FDA approved polymer.

In the example above, peptide cargo was conjugated to the polymer in a solution phase and resulting bioconjugates were used in the assembly of μS surfaces. To demonstrate conjugation and immobilization of oligopeptides within a matrix of PVA hydrogel, μS hydrogels were prepared using a 12 wt% solution of PVA$_{ER}$ as described above and incubated in a solution of GSH (2 mole equivalents to the total thiol content within the gel). Raw data were used to estimate reaction conversion as a function of time (**Figure 8**) which revealed a completion of conjugation, i.e. conversion of all the available polymer terminal groups into polymer-peptide conjugates, within 2 h of reaction. Inasmuch as thiol-disulfide exchange is expected to be largely insensitive to amino acid sequences of the thiol-containing oligopeptides, this experiment provides proof-of-concept immobilization of oligopeptides for diverse biotechnological and biomedical applications. We note that Figure 8 does not provide information on the localization of the cargo after, e.g., 40 minutes of reaction and a 50% conversion. However, a full conversion reached at 2 hours implies that at this time point, peptide immobilization occurs throughout the hydrogel and considers both, hydrogel bulk and the surface.

Next, μS thin films were prepared using PVA$_{ER}$ and used to achieve hydrogel functionalization through bioconjugation with c(RGDfC). Resulting samples were used as substrates for cell adhesion with analysis conducted as described above, **Figure 9**. In these experiments, to illustrate broader scope of the developed techniques, we used another mammalian cell line, human umbilical vein endothelial cells (HUVEC). In agreement with the data presented above, HUVEC revealed limited cell count on μS PVA films prepared using pristine PVA, amine- and ER- terminated polymer samples as well as GSH-polymer conjugate. On the other hand, PVA$_{RGD}$ conjugate formulated into a μS film and μS PVA$_{ER}$ hydrogel reacted with c(RGDfC) sustained a pronounced cell adhesion. Pre-conjugated sample exhibited a statistically significant higher cell count, however the magnitude of this effect

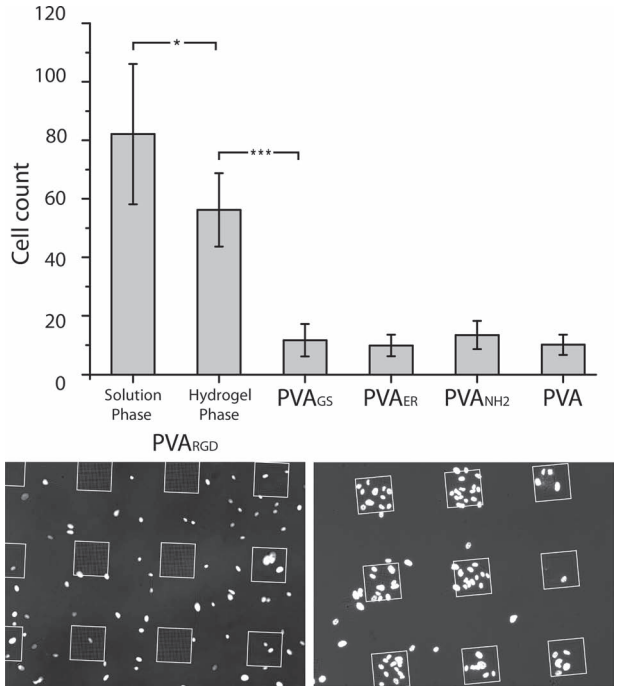

Figure 9. Top: Experimental values of cell counts of HUVEC cells on µS PVA films. The data are presented as mean values (triplicates) ± SD (n = 3). *** is $p < 0.005$; * is $p < 0.1$. Bottom: Fluorescence microscopy images of DAPI-stained HUVEC cells cultured on µS PVA_{RGD} films obtained using µTM and PVA_{RGD} conjugate (left) or via µTM using PVA_{ER} and hydrogel phase conjugation with c(RGDfC). Scale bars: 100 µm.

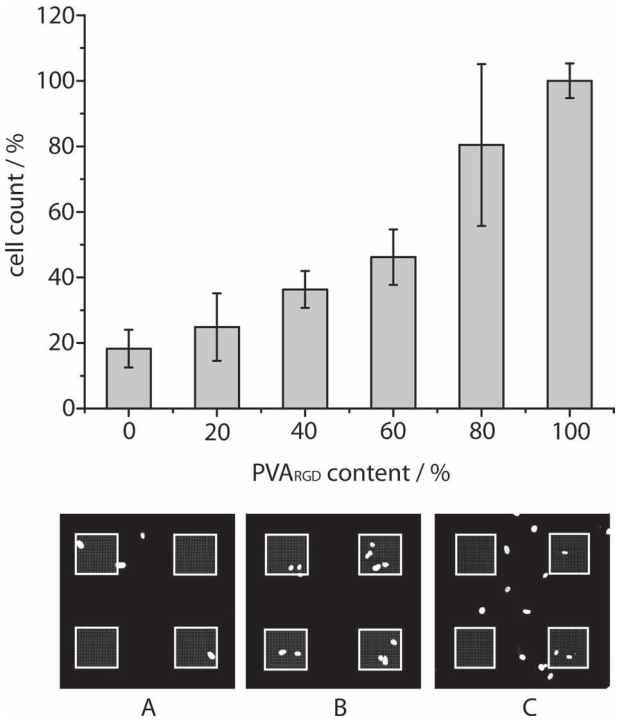

Figure 10. Top: Experimental values of cell counts of HUVEC on µS PVA hydrogels prepared using mixtures of PVA_{RGD} and PVA_{NH2}. The data are presented as mean values (triplicates) ± SD (n = 3). Bottom: Fluorescence microscopy images of DAPI-stained HUVEC cells cultured on hydrogels prepared using polymer mixtures with 20% (a), 40% (b), and 60% (c) of PVA_{RGD}. Scale bars: 100 µm.

was minor. A more pronounced difference between the samples was revealed upon a visual observation of the adhered cells. For pre-conjugated polymer, cell adhesion was uniform with no clear tendency for cells to occupy the µS surfaces. In stark contrast, adhesion of cells on post-conjugated samples proceeded with predominant localization of cells on the µS areas and resulted in cell patterning, Figure 9. This observation is intriguing in that chemical cues and topography design for the two surfaces were identical, yet resulting adhesion pattern for mammalian cells was vastly different. A plausible explanation to this phenomenon relates to the density and distribution of the RGD ligands achieved on µS surfaces with pre- and post- conjugation. We are currently investigating this patterning strategy in detail.

To further demonstrate opportunities in functionalization of hydrogels and control over deliverable payload or density of ligands, we capitalized on the data in Figure 5, which demonstrated co-gelation of a mixture of PVA chains. We revealed that a judicious choice of the ratio between PVA_{NH2} and PVA_{ER} taken for the production of µS hydrogels defines the available thiol conjugation sites. A similar approach can be used to design hydrogel matrices with controlled amount of incorporated chemical stimulus. Towards this end, we used mixtures of RGD-functionalized PVA (PVA_{RGD}) with peptide-free polymer (PVA_{NH2}) and quantified adhesion of HUVEC onto µS substrates prepared using these polymer mixtures. With increasing RGD content, we observed a gradual increase in the number of adhered cells (**Figure 10**). This outcome as such is expected, yet in the context of PVA hydrogels it has a deeper meaning in that it demonstrates a controllable incorporation of chemical function into non-functional gels. We envision that this approach will afford controlled functionalization using peptide cargo for guided cell adhesion and other TE applications,[59] which is a subject of our ongoing research. From a different perspective, we also observed that variation of PVA_{RGD} content in the polymer mixture has an effect similar to that discussed above using data in Figure 9, namely cell patterning. Specifically, a progressive increase in cell count observed upon an increase in PVA_{RGD} fraction from 20 to 40 and further to 60% is also accompanied by a change in the cell adhesion pattern. In particular, ligand density created with 60% of PVA_{RGD} favored uniform adhesion of HUVEC with no discernible pattern of cell anchorage. In contrast, at 40% of PVA_{RGD} the cells demonstrated a clear tendency of localization on µS areas of the surface, plausibly due to a higher local concentration of the pro-cell adhesive ligand, c(RGDfC). We note that for the discussed samples, the total cell count remains rather low (see fluorescence microscopic images), which is readily explained by insufficient density of RGD ligands.

3. Conclusion

In this work, we developed bioconjugation of oligopeptides to a gel forming, FDA approved polymer, PVA. We achieved site-specific conjugation through polymer terminal groups,

NANO MICRO small

for which purpose we elaborated on macromolecular design of PVA, specifically through polymer synthesis via RAFT and conversion of PVA terminal groups into sites for bioconjugation. We then achieved conjugation of peptide cargo employing polymer chains in solution and within the μS hydrogels at physiological solutions. Towards creation of functional biointerfaces, we (i) achieved assembly of surface-adhered μS PVA thin films and quantified the available conjugations sites within the hydrogels, (ii) demonstrated quantitative kinetic data on peptide conjugation to the polymer chains within the hydrogel phase and (iii) quantified success of bioconjugation through the use of cell-adhesive peptide and visualization of cell adhesion on PVA hydrogels as cell culture substrates. We envision that the developed techniques will significantly broaden utility of PVA in biomedicine and render the physical hydrogels derived thereof attractive for advanced biomedical applications, specifically co-culture of mammalian cells and tissue engineering.

4. Experimental Section

Materials: Unless stated otherwise, all chemicals and materials were purchased from Sigma-Aldrich and used as received without purification. Cyclo arginine-glycine-aspartate c(RGDfC) sequence was purchased from Anaspec (USA). The molecular weight and polydispersity index of custom-made PVA_{NH2} was 28 kDa and 1.16 respectively.[43] A sample of PVA with FITC labeling was obtained as described in details elsewhere.[23] High-purify water with a resistivity of 18 MΩ cm (MilliQ, MQ) was obtained from an in-line Millipore Synergy system (Millipore Corporation, U.S.A.).

Methods: Absorbance measurements were performed using UV-vis spectrophotometer (NanoDrop). Quantification of solution fluorescence was performed using an EnSpire Perkin Elmer multi-label plate reader. Differential interference contrast (DIC) and fluorescence microscopy images were obtained using a Zeiss Axio Observer Z1 microscope. Gel permeation chromatography (GPC) was performed using a system comprising a LC-20AD Shimadzu HPLC pump, a Shimadzu RID-10A refractive index detector and a DAWN HELEOS 8 light scattering detector along with a SPD-M20A PDA detector, equipped with a HEMA-Bio Linear column with 10 μm particles, a length of 300 mm and an internal diameter of 8 mm from MZ-Analysentechnik providing an effective molecular weight range of 1000–1 000 000.

Stamp Fabrication: The polydimethylsiloxane (PDMS) elastomer and curing agent (Sylgard 184, Dow Corning Corporation, USA) were mixed in a ratio of 10:1, degassed, and poured over silicon wafers patterned with SU-8 2002 photoresist structures (MicroChem, Newton, MA). The PDMS was cured for 3 h at 80 °C.

Preparation of Thiol-Activated PVA (PVA_{ER}): PVA sample with a M_n of 28 kDa was modified through the amine functionality with 2-iminothiolane (Traut's Reagent) and 5,5-dithiobis-(2-nitrobenzoic acid) (Ellmans's Reagent, ER). In particular, PVA (500 mg, 0.018 mmol) was dissolved in 5.5 mL carbonate buffer (0.1 M; pH 8.3) by heating to 90 °C for 3 h. The solution was cooled to room temperature (RT) and Traut's Reagent (20 mg, 0.14 mmol in 1 mL of buffer) was added, and a solution of ER (6.8 mg, 0.17 mmol in 3 mL of buffer) was added shortly afterwards, upon which the reaction mixture turned orange. The mixture was allowed to stir at RT for 40 h. The mixture was filtered and precipitated into methanol. The precipitate was collected by suction filtration and washed with methanol and diethylether to yield the PVA_{ER} as a white powder (460 mg, 92%).

Microtransfer Molding (μTM) of PVA_{ER}: Surface-adhered microstructured (μS) PVA_{ER} films were obtained via μTM. Typically, PVA_{ER} was dissolved in MQ water at 80 °C for at least 1 h. Polymer solution was cooled down to 37 °C prior to use. Subsequently, PVA_{ER} solution was placed between a glass cover slip and a PDMS stamp, and clamped together at finger-tight pressure overnight, after which the stamp was removed to afford a cover slip-adhered μS PVA_{ER} film. PVA_{ER} μS were then treated with 1 M of sodium sulfate (Na_2SO_4) "salting out" solution for 1 h, 1 h incubation in PBS (10 mM; pH 7) and finally washed with PBS buffer prior to analysis or subsequent procedure.

Thiol Content Based on the Concentrations of PVA_{ER} Solution: μS PVA_{ER} films were prepared with varying concentrations from 2 to 18 wt% PVA_{ER} solutions. 20 μL of DL-dithiothreitol (DTT) (50 g L^{-1} in PBS) was added to each sample and incubated for 2 min. Disulfide cleavage is confirmed by measuring absorbance of released 2-nitro-5-mercaptobenzoic acid (TNB) chromophore at 412 nm by Nanodrop.

Thiol Content Based on the% of PVA_{ER} Against PVA_{NH2} Solution: μS PVA films were prepared with 12 wt% PVA solutions varying in percentage of thiol-functionalized polymer (PVA_{ER}) against non-functionalized polymer (PVA_{NH2}). 20 μL of DTT (50 g L^{-1} in PBS) was added to each sample and UV-vis measurement was carried out on Nanodrop.

Efficiency of Thiol-Disulfide Exchange: μS PVA films were prepared using12 wt% PVA_{ER} solutions. To observe the kinetic reaction within μS hydrogel, reduced L-glutathione (GSH) in 2:1 mol ratio against PVA_{ER} was added to and incubated with μS PVA_{ER} films. Thiol-disulfide exchange was confirmed by measuring absorbance of released TNB choromophore at 412 nm.

Preparation of RGD-Conjugated PVA (PVA_{RGD}): 10.4 mg of PVA_{ER} was heated at 80 °C to dissolve in 86 μL of MQ. PVA_{ER} solution was diluted to 10 g L^{-1} in PBS buffer and added 0.17 mg of c(RGDfC) sequence (10 g L^{-1} in carbonate buffer). The reaction was allowed to proceed overnight and thiol-disulfide exchange was confirmed by measuring absorbance of released TNB choromophore at 412 nm. The reaction mixture was then purified via a size exclusion chromatography (SEC) using NAP-25 desalting column (GE Healthcare, UK) and freeze-dried to obtain white powder of PVA_{RGD} (8.6 mg, 82.7%).

Fabrication of μS PVA_{RGD} Films for Cell Immobilization: Pre-conjugated PVA_{RGD} μS films with 12 wt% and varying percentages of PVA_{RGD} were prepared as described above. Fabrication of post-conjugated PVA_{RGD} μS films was first prepared with 12 wt% PVA_{ER} solutions. 40 μL of c(RGDfC) (0.08 g L^{-1} in PBS buffer) was added to and incubated with μS PVA films after treatment of Na_2SO_4 solution for at least 2 h. Thiol-disulfide exchange is confirmed by measuring absorbance of released TNB choromophore at 412 nm and 100% of reaction was observed after 1 h of incubation.

Cell Immobilization on μS PVA Films: HepG2 (human hepatocellular carcinoma, Sigma-Aldrich) cancer cells and HUVEC*p* (human umbilical vein endothelial cells, *pooled,* Invitrogen) in cell growth media (DMEM & 10% FBS and medium 200 respectively) were incubated with sterilized μS PVA films for 24 h at 37 °C with 5% CO_2. Subsequently, μS PVA films were washed with PBS (3×)

to remove free cells and immobilized cells were fixed on μS PVA films with 4% of paraformaldehyde (PFA) for 20 min. μS PVA films were then washed with PBS (2×), incubated in T-PBS (0.1% Triton × 100 in PBS) for 15 min, and 2 wt% of albumin from bovine serum (BSA) in T-PBS for 2 h. μS PVA films were then washed with T-PBS (3×) and incubated with 4',6-diamidino-2-phenylindole dihydrochloride (DAPI) (0.01 g L^{-1} in PBS) for 1 h. After that, μS PVA films were then washed with T-PBS (3×) and PBS (3×) and observed under fluorescence microscopy.

Acknowledgements

This work is financed by the Lundbeck Foundation and Sapere Aude Starting Grant from the Danish Council for Independent Research, Technology and Production Sciences, Denmark.

[1] M. M. Stevens, J. H. George, *Science* **2005**, *310*, 1135.
[2] J. Engler, S. Sen, H. L. Sweeney, D. E. Discher, *Cell* **2006**, *126*, 677.
[3] J. Y. Wong, J. B. Leach, X. Q. Brown, *Surf. Sci.* **2004**, *570*, 119.
[4] J. D. Mendelsohn, S. Y. Yang, J. Hiller, A. I. Hochbaum, M. F. Rubner, *Biomacromolecules* **2003**, *4*, 96.
[5] P. Krsko, T. E. McCann, T. T. Thach, T. L. Laabs, H. M. Geller, M. R. Libera, *Biomaterials* **2009**, *30*, 721.
[6] M. Lo, H. B. Wang, M. Dembo, Y. L. Wang, *Biophys. J.* **2000**, *79*, 144.
[7] L. Kocgozlu, M. Rabineau, G. Koenig, Y. Haikel, P. Schaaf, J. N. Freund, J. C. Voegel, P. Lavalle, D. Vautier, *Biomaterials* **2012**, *33*, 798.
[8] L. Kocgozlu, P. Lavalle, G. Koenig, B. Senger, Y. Haikel, P. Schaaf, J. C. Voegel, H. Tenenbaum, D. Vautier, *J. Cell Sci.* **2010**, *123*, 29.
[9] H. J. Kong, S. Hsiong, D. J. Mooney, *Nano Lett.* **2007**, *7*, 161.
[10] T. Boudou, T. Crouzier, C. Nicolas, K. Ren, C. Picart, *Macromol. Biosci.* **2011**, *11*, 77.
[11] M. T. Thompson, M. C. Berg, I. S. Tobias, M. F. Rubner, K. J. Van Vliet, *Biomaterials* **2005**, *26*, 6836.
[12] N. M. Alves, I. Pashkuleva, R. L. Reis, J. F. Mano, *Small* **2010**, *6*, 2208.
[13] D. Aydin, V. C. Hirschfeld-Warneken, I. Louban, J. P. Spatz, in *Intelligent Surfaces in Biotechnology*, John Wiley & Sons, Inc., NY **2012**, p.291.
[14] H. J. Kong, J. D. Liu, K. Riddle, T. Matsumoto, K. Leach, D. J. Mooney, *Nat. Mater.* **2005**, *4*, 460.
[15] W. W. Ahmed, T. Wolfram, A. M. Goldyn, K. Bruellhoff, B. A. Rioja, M. Moller, J. P. Spatz, T. A. Saif, J. Groll, R. Kemkemer, *Biomaterials* **2010**, *31*, 250.
[16] J. Fukuda, A. Khademhosseini, J. Yeh, G. Eng, J. J. Cheng, O. C. Farokhzad, R. Langer, *Biomaterials* **2006**, *27*, 1479.
[17] H. J. Kong, D. J. Mooney, *Nat. Rev. Drug Discov.* **2007**, *6*, 455.
[18] A. F. Adler, A. T. Speidel, N. Christoforou, K. Kolind, M. Foss, K. W. Leong, *Biomaterials* **2011**, *32*, 3611.
[19] S. R. Khetani, S. N. Bhatia, *Nat. Biotechnol.* **2008**, *26*, 120.
[20] S. N. Bhatia, U. J. Balis, M. L. Yarmush, M. Toner, *FASEB J.* **1999**, *13*, 1883.
[21] I. Levental, P. C. Georges, P. A. Janmey, *Soft Matter* **2007**, *3*, 299.
[22] B. E. B. Jensen, M.-H. Alves, B. Fejerskov, B. Stadler, A. N. Zelikin, *Soft Matter* **2012**, *8*, 4625.
[23] B. E. B. Jensen, A. A. A. Smith, B. Fejerskov, A. Postma, P. Senn, E. Reimhult, M. Pla-Roca, L. Isa, D. S. Sutherland, B. Stadler, A. N. Zelikin, *Langmuir* **2011**, *27*, 10216.
[24] B. Fejerskov, B. E. B. Jensen, N. B. S. Jensen, S.-F. Chong, A. N. Zelikin, *ACS Appl. Mater. Interf.* **2012**, *4* 4981.
[25] B. Fejerskov, A. N. Zelikin, *PLoS One* **2012,** *7*, e49619.
[26] L. Hosta-Rigau, B. E. B. Jensen, K. S. Fjeldsø, A. Postma, G. Li, K. N. Goldie, F. Albericio, A. N. Zelikin, B. Städler, *Adv. Healthcare Mater.* **2012**, *1*, 791.
[27] K. H. Schmedlen, K. S. Masters, J. L. West, *Biomaterials* **2002**, *23*, 4325.
[28] C. M. Hassan, N. A. Peppas, *Adv. Polym. Sci.* **2000**, *153*, 37.
[29] M. H. Alves, B. E. B. Jensen, A. A. A. Smith, A. N. Zelikin, *Macromol. Biosci.* **2011**, *11*, 1293.
[30] L. Cao, D. J. Mooney, *Adv. Drug Deliv. Rev.* **2007**, *59*, 1340.
[31] K. Ladewig, *Expert Opin. Drug. Deliv.* **2011**, *8*, 1175.
[32] W. M. Saltzman, W. L. Olbricht, *Nat. Rev. Drug Discov.* **2002**, *1*, 177.
[33] E. Chiellini, A. Corti, S. D'Antone, R. Solaro, *Progr. Polym. Sci.* **2003**, *28*, 963.
[34] M. I. Baker, S. P. Walsh, Z. Schwartz, B. D. Boyan, *J. Biomed. Mater. Res. B: Appl. Biomater.* **2012**, *100B*, 1451.
[35] Y. Kojima, H. Maeda, *J. Bioact. Compat. Polym.* **1993**, *8*, 115.
[36] Y. Y. Tong, R. Wang, N. Xu, F. S. Du, Z. C. Li, *J. Polym. Sci. Pol. Chem.* **2009**, *47*, 4494.
[37] S. N. S. Alconcel, A. S. Baas, H. D. Maynard, *Polym. Chem.* **2011**, *2*, 1442.
[38] B. Le Droumaguet, J. Nicolas, *Polym. Chem.* **2010**, *1*, 563.
[39] P. J. Roth, C. Boyer, A. B. Lowe, T. P. Davis, *Macromol. Rapid Comm.* **2011**, *32*, 1123.
[40] G. Moad, E. Rizzardo, S. H. Thang, *Polym. Int.* **2011**, *60*, 9.
[41] A. N. Zelikin, G. K. Such, A. Postma, F. Caruso, *Biomacromolecules* **2007**, *8*, 2950.
[42] Z. C. Li, Y. Y. Tong, Y. Q. Dong, F. S. Du, *J. Polym. Sci. Pol. Chem.* **2009**, *47*, 1901.
[43] A. A. Smith, T. Hussmann, J. Elich, A. Postma, M.-H. Alves, A. N. Zelikin, *Polym. Chem.* **2012**, *3*, 85.
[44] M. G. Cascone, B. Sim, S. Downes, *Biomaterials* **1995**, *16*, 569.
[45] J. E. Gough, C. A. Scotchford, S. Downes, *J. Biomed. Mater. Res.* **2002**, *61*, 121.
[46] D. A. Ossipov, J. Hilborn, *Macromolecules* **2006**, *39*, 1709.
[47] D. A. Ossipov, K. Brännvall, K. Forsberg-Nilsson, J. Hilborn, *J. Appl. Polym. Sci.* **2007**, *106*, 60.
[48] G. Saito, J. A. Swanson, K. D. Lee, *Adv. Drug Deliv. Rev.* **2003**, *55*, 199.
[49] S. Lofthouse, *Adv. Drug Deliv. Rev.* **2002**, *54*, 863.
[50] H. J. Griesser, H. Hall, T. A. Jenkins, S. S. Griesser, K. Vasilev, in *Intelligent Surfaces in Biotechnology*, John Wiley & Sons, Inc, NY **2012**, p.183.
[51] X. X. Zhang, H. S. Eden, X. Y. Chen, *J. Control. Release* **2012**, *159*, 2.
[52] J. Jackman, N.-J. Cho, *Biointerphases* **2012**, *7*, 1.
[53] A. Khademhosseini, R. Langer, *Biomaterials* **2007**, *28*, 5087.
[54] T. R. Hoare, D. S. Kohane, *Polymer* **2008**, *49*, 1993.
[55] B. V. Slaughter, S. S. Khurshid, O. Z. Fisher, A. Khademhosseini, N. A. Peppas, *Adv. Mater.* **2009**, *21*, 3307.
[56] R. V. Ulijn, N. Bibi, V. Jayawarna, P. D. Thornton, S. J. Todd, R. J. Mart, A. M. Smith, J. E. Gough, *Mater. Today* **2007**, *10*, 40.
[57] E. Ruoslahti, *Annu. Rev. Cell Dev. Bi.* **1996**, *12*, 697.
[58] S.-F. Chong, A. Sexton, R. De Rose, S. J. Kent, A. N. Zelikin, F. Caruso, *Biomaterials* **2009**, *30*, 5178.
[59] Y. Ito, *Soft Matter* **2008**, *4*, 46.

Received: July 24, 2012
Published online: December 3, 2012

